Vol. 92 No. 4 pp. 1667–1669 ACTA GEOLOGICA SINICA (English Edition) Aug. 2018

Research Advances

REE Characteristics of a New Uranium Mineral from the Xianshi Uranium Deposit, South China

LUO Jincheng[1, 2, *], HU Ruizhong[1], BI Xianwu[1] and CHEN Youwei[1]

1 *State Key Laboratory of Ore Deposit Geochemistry, Institute of Geochemistry, Chinese Academy of Sciences, Guiyang 550081, China*

2 *Department of Geological Sciences, University of Manitoba, Winnipeg R3T 2N2, Canada*

Objective

Galuskin et al. (2011) firstly discovered that vorlanite ($CaU^{6+/4+}$)O_4 is a rare Ca-rich mineral with a fluorite-type structure, which is isostructural with uraninite ($U^{4+}O_2$). Previous studies of the Xianshi granite-related uranium deposit reported that uraninite and pyrite are the major ore minerals whereas galena, clausthalite (PbSe), and pyrite are minor phases in the ores. A more detailed petrographic and geochronological study of the uranium minerals from the Xianshi deposit showed that there are three distinct types of uraninite-bearing assemblages which formed at three mineralization episodes (Fig. 1a; Luo et al., 2015).

Luo et al (2015) initially identified the main ore mineral as uraninite. However, they did note that chemistry was inconsistent with pure uraninite because of the high Ca values and suggested the high-Ca uraninite could be vorlanite. Therefore, the objective of this study is to characterize the main uranium ore mineral from the Xianshi uranium deposit, South China using LA-ICP-MS analytical technique.

Methods

Rare earth elements (REEs) concentrations in uranium minerals were determined using a New Wave laser ablation system with a wavelength of 213 nm connected to a Thermo Finnigan Element2 high resolution sector field ICP-MS at the University of Manitoba. Ablation was carried out at laser energy densities of 1.5–3.0 J/cm^2 with a beam diameter of 20 μm and a repetition rate of 5 Hz. Integration time was set to 15 ms for all elements except for ^{43}Ca and ^{238}U for which 10 and 5 ms, respectively, were chosen. The concentrations of the following isotopes were measured: ^{139}La, ^{140}Ce, ^{141}Pr, ^{143}Nd, ^{147}Sm, ^{151}Eu, ^{157}Gd, ^{159}Tb, ^{163}Dy, ^{165}Ho, ^{166}Er, ^{169}Tm, ^{173}Yb, ^{175}Lu. Element concentrations, lower limits of detection and errors (1σ) were calculated using the GLITTER software (Version 3.0), with NIST SRM 610 as an external standard and ^{235}U as an internal standard. This could introduce a small error concerning the absolute REE concentrations, but relative patterns and element ratios are not affected. Standard deviations (1σ) for REEs are 3%–4% for uranium mineral analyses.

Results

Analytical results of LA-ICP-MS for the Xianshi uranium mineral grains from different episodes are presented in the Appendix 1. In general, the Xianshi uranium mineral grains from three episodes of mineralization show similar normalized REE patterns (Fig. 1b). However, some REEs such as La, Eu, Dy, Yb and Lu have different contents for various episodes, varying up to three orders of magnitude (Fig. 1b). For example, uranium mineral grains from Episode I (135 Ma) have the highest REEs contents, whereas those from episode III (104 Ma) contain the lowest REEs. Those from episode II (113 Ma) have moderate REEs contents (Fig. 1b). Correspondingly, ∑REEs of episode I uranium mineral grains have the highest contents (~1711 to 4805 ppm), whereas those from episode III contain the lowest ∑REEs (~13 to 134 ppm). Episode II grains have moderate ∑REEs contents (~212 to 1621 ppm).

Notably, most of those uranium mineral grains show slightly positive Eu anomalies. Additionally, REE patterns of the Xianshi uranium mineral present obvious difference from those of the Sundong granite-hosted rocks, the Xianshi mafic dykes, granite-related uraninites, and other different types of uranium occurrences and deposits (Figs. 1b–e). Although the Xianshi uranium deposit has the same wall rock as those granite-related uranium deposits, LA–ICP–MS REEs results for uranium mineral probably indicate that the Xianshi uranium mineral could not be uranium oxide (e.g., UO_2).

* Corresponding author. E-mail: luojincheng@mail.gyig.ac.cn

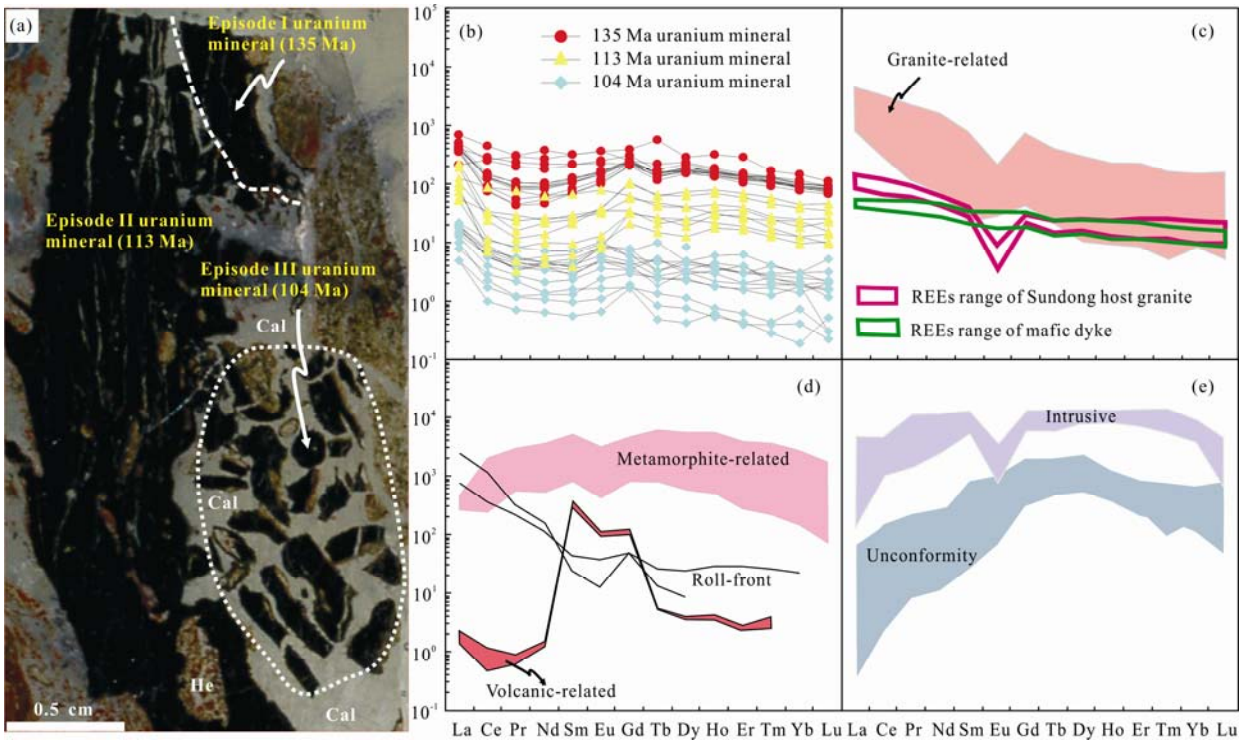

Fig. 1. (a), Three episodes of the Xianshi uranium mineral grains occur within a single thin section with calcite (Cal), hematite (He), and SIMS U-Pb ages (Luo et al., 2015); (b–e), Chondrite-normalized REE patterns of the Xianshi uranium mineral from three different episodes compared to the REE ranges obtained for uranium oxides from six different types of uranium occurrences (Mercadier et al., 2011), showing significant difference between the REE patterns of the Xianshi uranium mineral, the Xianshi mafic dykes, the Sundong host granite, those of granite-related uraninites, and other different types of uranium occurrences and deposits.

Conclusion

This study could explain why three episodes of uranium mineral from the Xianshi uranium deposit show distinct REEs compositions from various mineralization stages as demonstrated by SIMS uranium mineral U-Pb dating (Luo et al., 2015). More importantly, compared to the REE ranges obtained for uranium oxides from six different types of uranium occurrences, the Xianshi uranium deposit has the same wall rocks as those granite-related uranium deposits, indicating that the Xianshi uranium mineral could not be uranium oxide (e.g., UO_2). Therefore, the REE characteristics of the Xianshi uranium mineral probably supports that it could be vorlanite.

Acknowledgments

This work was supported by the National Key R&D Program of China (grant No. 2016YFC0600405), the Strategic Priority Research Program (B) of CAS (grant No. XDB18030202), the Natural Science Foundation of China (41603051), the Key Program of Science and Technology of Guizhou (grant No. [2018]1423) and CSC program to Luo.

References

Galuskin, E.V., Armbruster, T., Galuskina, I.O., Lazic, B., Winiarski, A., Gazeev, V.M., Dzierzanowski, P., Zadov, A.E., Pertsev, N.N., Wrzalik, R., Gurbanov, A.G., Janeczek, J., 2011. Vorlanite (CaU^{6+}) O_4—A new mineral from the Upper Chegem caldera, Kabardino-Balkaria, Northern Caucasus, Russia. *American Mineralogist* 96: 188–196.

Luo, J.C., Hu, R.Z., Fayek, M., Li, C.S., Bi, X.W., Abdu, Y., Chen, Y.W., 2015. In-situ SIMS uraninite U–Pb dating and genesis of the Xianshi granite-hosted uranium deposit, South China. *Ore Geology Reviews* 65: 968–978.

Mercadier, J., Cuney, M., Lach, P., Boiron, M.C., Bonhoure, J., Richard, A., Leisen, M., Kister, P., 2011, Origin of uranium deposits revealed by their rare earth element signature. *Terra Nova* 23: 264–269.

Appendix 1 LA–ICP–MS results for REEs (ppm) in uranium mineral grains from the Xianshi uranium deposit, South China

Sample	La	Ce	Pr	Nd	Sm	Eu	Gd	Tb	Dy	Ho	Er	Tm	Yb	Lu
Episode I (135 Ma)														
XS-28	377.64	79.41	46.42	56.66	71.83	111.21	214.11	146.52	161.81	158.13	135.29	108.04	92.82	80.55
XS-29	403.80	132.35	91.58	93.58	110.46	149.83	235.52	160.70	174.41	159.54	138.37	114.12	92.94	83.86
XS-30	434.60	133.50	88.42	88.01	111.11	160.00	259.37	156.15	194.09	168.55	139.40	126.67	104.00	94.49
XS-31	428.69	124.67	82.32	83.08	105.23	150.86	248.18	150.53	187.01	162.54	135.65	120.00	96.53	86.06
XS-32	469.62	153.59	107.37	105.57	125.49	171.90	250.61	162.03	181.10	160.78	128.76	110.59	90.59	74.80
XS-34	718.99	452.61	321.05	387.58	323.53	370.69	399.51	580.21	296.46	323.32	300.30	170.20	148.24	112.60
XS-35	217.30	266.34	302.11	276.23	324.84	368.97	254.01	224.60	240.55	189.40	154.08	135.29	118.82	94.49
XS-36	408.44	292.48	238.95	226.98	222.22	233.97	222.38	168.98	167.32	134.98	108.16	92.94	78.00	70.08
XS-37	356.96	75.65	43.79	47.00	71.63	102.41	211.68	116.58	157.48	139.22	117.64	107.84	88.00	75.59
XS-38	399.16	143.79	111.58	99.36	129.41	160.34	239.42	136.36	182.68	144.52	122.72	116.86	93.53	83.86
XS-39	524.47	256.54	203.16	181.16	218.30	258.62	312.90	180.48	229.13	178.27	145.02	133.73	106.76	92.91
XS-40	383.97	94.44	56.53	63.81	83.73	123.28	235.52	133.69	172.83	152.47	124.47	115.29	86.59	81.50
XS-41	445.15	137.09	94.11	92.93	121.83	167.93	270.07	156.95	197.64	173.67	142.60	130.20	103.76	95.12
Episode II (113 Ma)														
XS-02	129.54	91.34	77.89	64.88	69.93	82.76	64.23	42.51	40.94	33.04	26.53	25.10	24.06	16.02
XS-03	200.00	25.33	12.42	14.50	22.16	39.14	109.00	64.44	77.56	80.74	71.78	60.78	45.47	46.85
XS-04	231.65	34.69	16.84	22.57	26.21	39.48	102.58	65.51	65.24	72.26	60.79	47.65	40.18	35.75
XS-05	107.59	31.86	24.21	27.84	27.45	32.59	58.39	48.93	41.73	46.29	41.69	28.63	26.24	26.85
XS-06	76.92	11.76	8.53	10.49	9.87	13.62	32.70	28.05	26.06	35.62	37.04	25.61	19.35	23.35
XS-07	91.98	7.27	3.38	4.54	4.05	8.41	32.70	27.27	19.69	30.57	29.67	18.24	13.18	14.45
XS-08	89.87	39.38	33.68	37.26	36.54	45.69	53.53	81.28	39.76	50.53	53.78	27.02	26.18	22.36
XS-09	300.84	163.89	121.79	128.48	105.23	119.48	119.71	174.87	83.07	86.93	85.20	49.41	44.35	38.43
Episode III (104 Ma)														
XS-12	5.02	1.05	0.73	0.66	0.58	0.69	1.70	0.51	0.44	0.65	0.41	0.42	0.44	0.24
XS-13	8.19	2.97	2.28	1.46	1.67	1.72	1.75	1.42	1.17	0.80	0.63	0.46	0.75	0.31
XS-14	15.99	7.70	5.89	4.75	5.49	8.64	6.13	3.34	4.49	3.76	3.05	4.08	3.18	3.31
XS-15	20.42	7.43	4.83	3.85	3.57	4.97	4.23	1.90	3.27	2.23	2.01	2.00	2.00	0.31
XS-16	20.34	8.15	5.39	4.82	4.59	9.16	8.08	3.37	5.16	4.01	3.20	3.02	3.19	2.20
XS-17	20.68	6.11	3.87	4.80	3.92	9.14	7.49	10.43	4.96	6.18	6.47	4.31	3.18	5.35
XS-18	17.72	6.05	3.79	4.07	2.81	5.52	4.33	5.35	3.54	4.66	3.99	2.47	2.18	1.22
XS-19	18.40	5.85	3.83	3.55	3.01	4.90	3.65	5.43	3.03	3.37	4.17	2.20	1.89	1.69
XS-20	5.05	1.76	1.23	1.11	1.01	1.14	2.00	0.88	0.79	0.56	0.46	0.30	0.19	0.55
XS-21	13.08	4.10	2.85	2.18	2.42	3.72	3.50	2.46	2.48	1.82	1.64	1.80	1.46	2.09
XS-22	14.68	6.24	4.64	4.22	4.23	6.31	4.87	2.75	3.35	3.09	2.07	2.59	1.94	2.17
XS-23	22.74	11.62	8.86	7.39	7.25	10.79	5.99	4.68	4.84	3.83	3.02	2.90	2.58	2.36
XS-25	10.25	2.35	1.25	1.37	1.38	2.47	3.07	2.54	2.36	1.89	1.63	1.33	1.85	1.61